Available online at www.sciencedirect.com
ScienceDirect
Journal of Hazardous Materials 147 (2007) 979–985
Journal of Hazardous Materials
www.elsevier.com/locate/jhazmat

Adsorption characteristics of Congo Red onto the chitosan/montmorillonite nanocomposite

Li Wang [a,b], Aiqin Wang [a,*]

[a] Center of Eco-material and Green Chemistry, Lanzhou Institute of Chemical Physics, Chinese Academy of Sciences, Lanzhou 730000, PR China
[b] Graduate School of the Chinese Academy of Sciences, Beijing 100049, PR China

Received 26 June 2006; received in revised form 18 January 2007; accepted 26 January 2007
Available online 9 February 2007

Abstract

A series of biopolymer chitosan/montmorillonite (CTS/MMT) nanocomposites were prepared by controlling the molar ratio of chitosan (CTS) and montmorillonite (MMT). The nanocomposites were characterized by FTIR and XRD. The effects of different molar ratios of CTS and MMT, initial pH value of the dye solution and temperature on adsorption capacities of samples for Congo Red (CR) dye have been investigated. The adsorption capacities of CTS, MMT and CTS/MMT nanocomposite with CTS to MMT molar ratio of 5:1 for CR were compared. The results indicated that the adsorption capacity of CTS/MMT nanocomposite was higher than the mean values of those of CTS and MMT. The adsorption kinetics and isotherms were also studied. It was shown that all the sorption processes were better fitted by pseudo-second-order equation and the Langmuir equation.

Keywords: Chitosan; Montmorillonite; Nanocomposites; Adsorption; Congo Red

1. Introduction

Colored organic effluent is produced in industries such as textiles, rubber, paper, plastic, cosmetics, etc. Discharging of dyes into water resources even in a small amount can affect the aquatic life. Therefore, colored wastewater cannot be discharged without adequate treatment. As dyes are designed to resist breakdown with time and exposure to sunlight, water, soap, and oxidizing agent, they cannot be easily removed by conventional wastewater treatment processes due to their complex structure and synthetic origins [1]. Thus, dye removal has been an important but challenging area of wastewater treatment.

To remove dyes and other colored contaminants from wastewaters, several physical, chemical, physico-chemical and biological methods have been developed. Among these methods, adsorption has been found to be one of the most popular physico-chemical treatment methods for removing dyes with potential applications [2]. It has been reported that many different types of adsorbents are effective in removing color from aqueous effluent. Natural polymeric materials are gaining interest for application as adsorbents in wastewater treatment due to their biodegradable and non-toxic nature [3]. Chitosan (CTS) is the *N*-deacetylated derivative of chitin and the second most plentiful natural biopolymer. As a well-known sorbent, CTS is widely used for the removal of heavy, transition metals and dyes [4–6]. Nevertheless, the market cost of CTS is relative high and its specific gravity should be improved for practical operation. Therefore, several attempts have been made to develop cheaper and effective adsorbents.

Natural phyllosilicates, commonly known as clays considering their particle size, such as montmorillonite (MMT), have the potential to act as alternative low-cost adsorbents. Wang et al. compared the adsorption properties of basic dyes onto Ca-MMT and Ti-MMT and found that Ca-MMT possessed larger adsorption capacity than Ti-MMT because Ca^{2+} is easier to be displaced by ion exchange [7]. Özcan and Özcan reported that the removal of acid dyes was promoted using sulfuric acid-activated MMT compared with untreated MMT [8]. They showed that the modified clays displayed higher adsorption capacity than the original clay.

Polymer/layered silicate nanocomposites frequently exhibit remarkably improved mechanical and materials properties and are attracting considerable interest in polymer science field [9]. Wang et al. prepared chitosan/montmorillonite (CTS/MMT)

* Corresponding author. Tel.: +86 931 4968118; fax: +86 931 8277088.
E-mail address: aqwang@lzb.ac.cn (A. Wang).

0304-3894/$ – see front matter © 2007 Elsevier B.V. All rights reserved.
doi:10.1016/j.jhazmat.2007.01.145

nanocomposites and discovered that the flocculated–intercalated nanostructure formed at high MMT content and the intercalate-exfoliated nanostructure formed at low MMT content [10]. Darder et al. prepared CTS/MMT nanocomposites and used them in potentiometric sensors for the anionic detection [11,12]. Gecol et al. investigated the removal of tungsten from water using CTS/MMT nanocomposites [13]. However, the reports about the removal of dyes of CTS/MMT nanocomposites as an adsorbent are very scarce though Chang and Juang studied the adsorption of tannic acid, humic acid, and dyes (methylene blue, reactive dye RR222) from water using the composite of CTS and activated clay [3]. Therefore, a series of CTS/MMT nanocomposites were synthesized and characterized, and the adsorption kinetics and isotherms for Congo Red (CR) dye from water solution onto nanocomposite with CTS to MMT molar ratio of 5:1 were compared with those of CTS and MMT in this study. The effects of various experimental conditions, such as different molar ratios of CTS to MMT, initial pH value of the dye solution and adsorption temperature, have been investigated.

2. Experimental

2.1. Materials

The degree of deacetylation and a viscosity–average molecular weight of CTS (Zhejiang Yuhuan Ocean Biology Co., China) is 85% and 9.0×10^5, respectively. The cation exchange capacity (CEC) of MMT (Shandong Longfeng Montmorillonite Co., China) is 102.8 mequiv./100 g. The molecular weight of CR (Tianjin Kermel Chemical Reagent Co., China) is 696.66 g/mol. Other agents used were all analytical grade and all solutions were prepared with distilled water.

2.2. Preparation of the nanocomposites

The nanocomposites were prepared by the method of Wang et al. [10]. Four grams of MMT was swelled by 100 mL distilled water. CTS solution (containing CTS amounts of 0.0660, 0.132, 0.660, 3.30, 6.60 g) was prepared by dissolving CTS in 1% (v/v) aqueous acetic acid solution, and then the pH of the resulting solution was adjusted to 4.90 with 20 wt% NaOH solution, then CTS solution was slowly added to MMT suspension followed by stirring at 60 °C for 6 h to obtain nanocomposites with CTS to MMT molar ratios of 1:10, 1:5, 1:1, 5:1 and 10:1, respectively. The formed composites were washed with distilled water until the pH of the supernatant (fluid) reached 7.00, and then dried at 60 °C for 12 h. All samples were ground and sieved to 200 mesh size. The density of the samples was measured by stack density method.

2.3. Characterization

IR spectra of the samples were characterized using a FTIR Spectrophotometer (Thermo Nicolet, NEXUS, TM) in KBr pellets. XRD analyses of the powered samples were performed using an X-ray power diffractometer with Cu anode (PAN alytical Co. X'pert PRO), running at 40 kV and 30 mA, scanning from 4° to 18° at 3°/min. The surface area and pore size of the samples were measured using an Accelerated Surface Area and Porosimetry System (Micromeritics, ASAP 2010) by BET-method at 76 K.

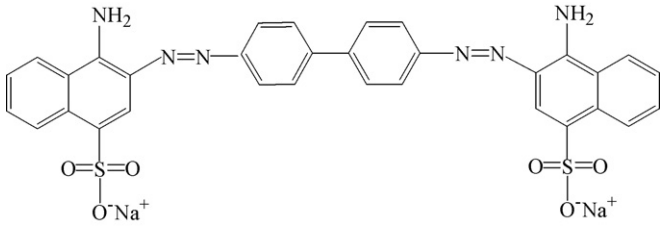

Fig. 1. Structure of CR (molecular formula: $C_{32}H_{22}N_6O_6S_2Na_2$).

2.4. Adsorption experiments

For the all batch adsorption experiments, were performed on a thermostated shaker (THZ-98A) with a shaking of 120 rpm. During the effect of molar ratios of CTS to MMT on adsorption capacities of CR experiments, 0.10 g of the nanocomposite and 25.00 mL of CR solution (initial concentration 200 mg/L, initial pH) were used. The system was maintained under shaking at 30 °C until adsorption equilibrium reached. The influence of pH on CR removal was studied by adjusting CR solutions (400 mg/L) to different pH values (4–9) using a pH meter (DELTA-320) and agitating 25.00 mL of dye solution with 0.10 g of adsorbent at 30 °C for 12 h. The effect of temperature on dye removal was carried out in the 25.00 mL of dye solutions (400 mg/L, pH 7.00) with 0.10 g of adsorbent for 12 h.

For kinetic study, 400 mg/L dye solutions (25.00 mL, pH 7) were agitated with 0.10 g of adsorbent at 30 °C for predetermined intervals of time. Batch equilibrium adsorption experiments were carried out by agitating 25.00 mL various dye concentrations of CR solution at pH 7 with 0.10 g of adsorbent at 30 °C until equilibrium was established.

The samples were withdrawn from the shaker at predetermined time intervals and the dye solution was separated from the adsorbent by centrifugation at 4500 rpm for10 min. The absorbencies of solution were measured using a UV–vis spectrophotometer (Specord, 200) at wavelength 500 nm. (CR has a maximum absorbency at wavelength 500 nm on a UV–vis spectrophotometer. The molecular structure of CR is shown in Fig. 1.) Then, the concentrations of the solutions were determined by using linear regression equation ($y = 0.0342x + 0.0698$, $R^2 = 0.9999$) obtained by plotting a calibration curve for dye over a range of concentrations. The amounts of CR adsorbed onto samples were calculated by subtracting the final solution concentration from the initial concentration of dye solutions.

3. Results and discussion

3.1. IR analysis of nanocomposites

IR spectra of MMT, CTS, and five nanocomposites with various molar ratios of CTS to MMT are shown in Fig. 2. It can be found the absorption band of the nanocomposites at

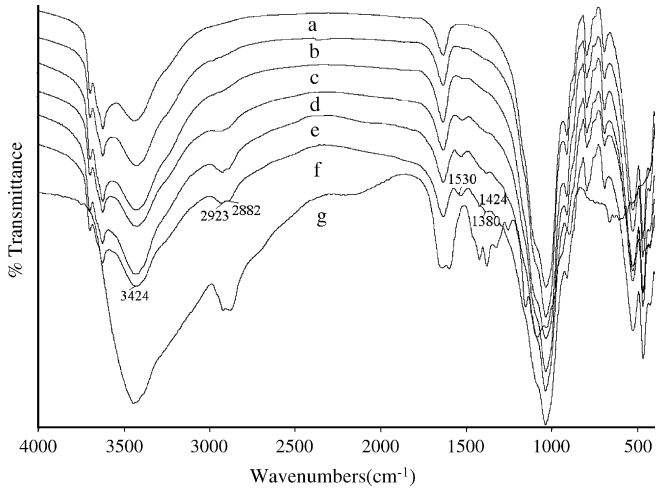

Fig. 2. IR spectra of the MMT (a), the nanocomposites with the molar ratios CTS to MMT of 1:10 (b), 1:5 (c), 1:1 (d), 5:1 (e), 10:1 (f) and CTS (g).

3424 cm^{-1} becomes enhancement, which suggests the vibration bands in CTS (O–H and N–H stretching) overlap with the bands of MMT (–OH stretching of H_2O). The bands attributed to the intercalated CTS (C–H stretching on methyl (2923 cm^{-1}) and methylene (2882 cm^{-1}) groups) are observed in the spectra of the nanocomposites, and the intensity of the both adsorption bands increased with increasing the molar ratio of CTS to MMT. In addition, the bands attributed to the intercalated CTS (C–H bending on methyl (1424 cm^{-1}) and methylene (1380 cm^{-1}) groups) are also observed in the spectra of the nanocomposites, and the intensity of the both adsorption bands increased with increasing the molar ratio of CTS to MMT. The intensity of the band at 1630 cm^{-1} increased, which indicates the first NH–CO group stretching vibration of CTS overlap with –OH bending vibration of H_2O of the MMT. The absorption band at 1530 cm^{-1}, attributed to the deformation vibration of the protonated amine group of CTS also becomes stronger with increasing the molar ratios of CTS to MMT. The information observed from IR spectra indicates that the molar ratio of CTS to MMT could influence chemical environment of the nanocomposites, and then may have an influence on absorption properties of the nanocomposites.

3.2. X-ray diffraction analysis of nanocomposites

Three nanocomposites with the molar ratios of CTS to MMT of 1:5, 1:1 and 5:1 was analysed by XRD and the powder patterns of MMT and nanocomposites are presented in Fig. 3. In acidic solutions, CTS shows an extended structure that may facilitate the biopolymer intercalation in the clay interlayer space in opposition to analogous polysaccharides with coiled or helicoidal structures that are only adsorbed in the external surface of clays [11]. A typical diffraction peak of MMT is 6.94°, responding to a basal spacing of 12.74 Å. After intercalation with CTS, this peak disappears. The movement of the typical diffraction peak of MMT to lower angle (5.61°) indicates the formation of the flocculated–intercalated nanostructure with the molar ratios CTS to MMT of 1:5. It is reported that the formation of flocculated structure in CTS/MMT nanocomposites is due to the hydroxylated edge–edge interaction of the silicate layers [14]. The intensity of the peak decreases and even disappears with increasing of the molar ratios of CTS to MTT indicated that the formation of an intercalated–exfoliated structure in CTS/MMT nanocomposites. According to the results of XRD and FTIR, it can be concluded that almost all CTS intercalated into MMT interlayer with destroying the crystalline structure of MMT.

3.3. Effect of molar ratios of CTS to MMT of nanocomposites on adsorption

As the molar ratios of CTS to MMT increases, CTS/MMT mixtures tend to shrink and which enhances the capability of CTS and MMT to agglomerate. This can facilitate the separation of the adsorbents from the solution, which is especially important for the practical applications. Fig. 4 shows the effect of molar ratios of CTS to MMT of the nanocomposites on adsorption capacity of CR. As seen from Fig. 4, the adsorption capacities of CR increase with increasing of the molar ratios of CTS to MMT, but the adsorption capacities increase slowly when the molar ratio of CTS to MMT exceeds 1:1. This is because increasing the amount of CTS is helpful to balance the initial negative charges of MMT and enhance the adsorption capacities of anion CR for the nanocomposites. So, it is found that the adsorption capacities of dye increase rapidly with increasing of the molar ratio of CTS to MMT from 1:10 to 1:1. However, the adsorption capacities increase slowly when the molar ratio of CTS to MMT exceeds 1:1, which is attributed to the amount of intercalated CTS is saturated.

To further support the explanation mentioned above, we also investigated the effect of molar ratio of CTS to MMT on the density, the surface area as well as the pore size of nanocomposites. The test results indicate, compared with MMT (1.56 g/m^3, 61.4 m^2/g), the density and the surface area of nanocomposites decrease with increasing of the molar ratio of CTS to MMT from 1:5 (1.52 g/m^3, 55.5 m^2/g) to 5:1 (1.39 g/m^3, 22.3 m^2/g).

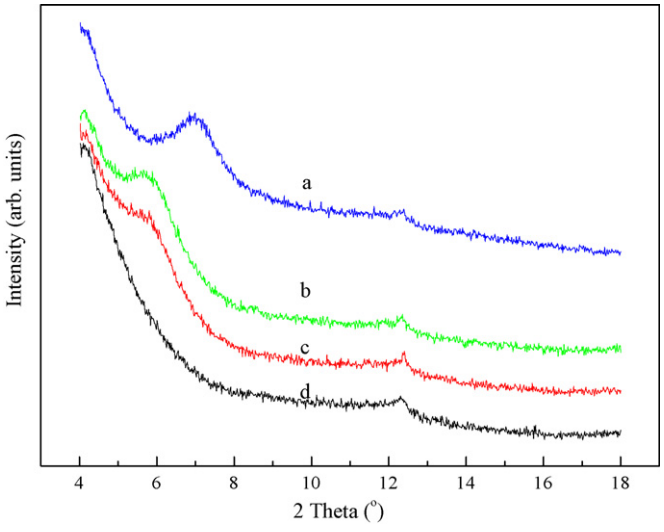

Fig. 3. XRD powder patterns of the MMT (a), the nanocomposites with the molar ratios of CTS to MMT of 1:5 (b), 1:1 (c) and 5:1 (d).

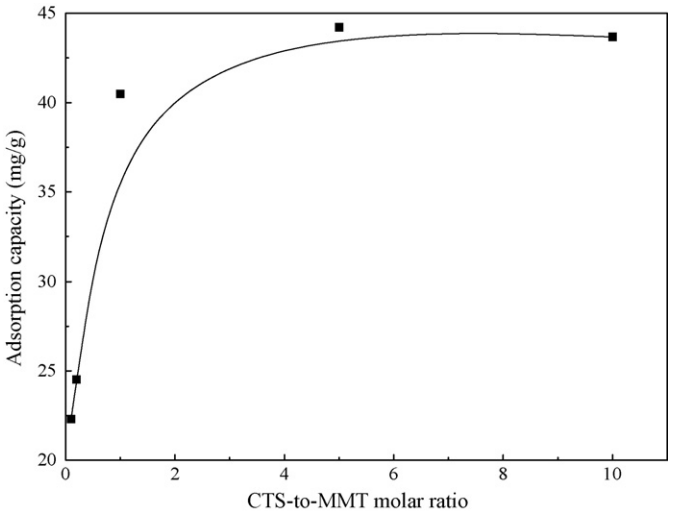

Fig. 4. Effect of the molar ratios of CTS to MMT on adsorption capacity of the nanocomposites for CR. Adsorption experiments—dye concentration: 200 mg/L; sample dose: 0.1 g/25.00 mL; natural pH; temperature: 30 °C; equilibrium time: 720 min.

However, the pore size of nanocomposites increase with increasing of the molar ratio of CTS to MMT from 1:5 (7.4 nm) to 5:1 (11.8 nm) by compared with MMT (6.7 nm). The synergic effects of these factors may be result in the higher adsorption capacity of nanocomposite with CTS to MMT molar ratio of 5:1 for CR dye. Therefore, the nanocomposite with the molar ratio of CTS to MMT was selected as 5:1 in this study.

3.4. Effect of pH value on adsorption

The pH value of the dye solution is an important factor for the determination the adsorption of solutes [15]. The influence of the pH value in the original solution on the adsorption capacity of dye is shown in Fig. 5. This result indicated that when the pH value of the dye solution was raised from 4 to 7 (it is worth pointing out that CR was slightly soluble in water at the pH 2), the adsorption capacity reduced from 96.62 to 74.73, 29.52 to 6.25 and 72.11 to 50.63 mg/g for CTS, MMT, and the nanocomposite, respectively, and then slowly decrease with the increasing of the pH from 7 to 9. At that, it is worth pointing out that the adsorption capacity of the nanocomposite is higher than the mean values of those of CTS and MMT at any pH, which help to reduce the market cost of CTS.

Two possible mechanisms of adsorption of CR may be considered: (a) electrostatic interaction between the protonated groups of CTS and the dye, and (b) the chemical reaction between the adsorbate and the adsorbent [16]. Given that the pK_a of the primary amine groups in the CTS structure is 6.3, an acidic pH value is necessary to provide $-NH_3^+$ groups in the CTS structure facilitating a increase of dye adsorption [12]. On the other hand, the anion dye sorption through exchange of ions is favored at low pH values especially when the sorption rate is largely controlled by ion exchange rather than by complexation [17]. At pH above 7, the excessive hydroxyl ions may compete with the dye anions and hence a slow reduction in dye uptake was observed. However, significant adsorption of the anionic dye on the adsorbent still occurred at alkaline pH values. This suggests that the chemisorption mechanism might be operative. Similar trend observed in the adsorption of CR on wollastonite [18], biogas residual slurry [19], banana pith [20], waste Fe(III)/Cr(III) hydroxide [21], waste orange peel [22], waste red mud [23] and activated carbon [16].

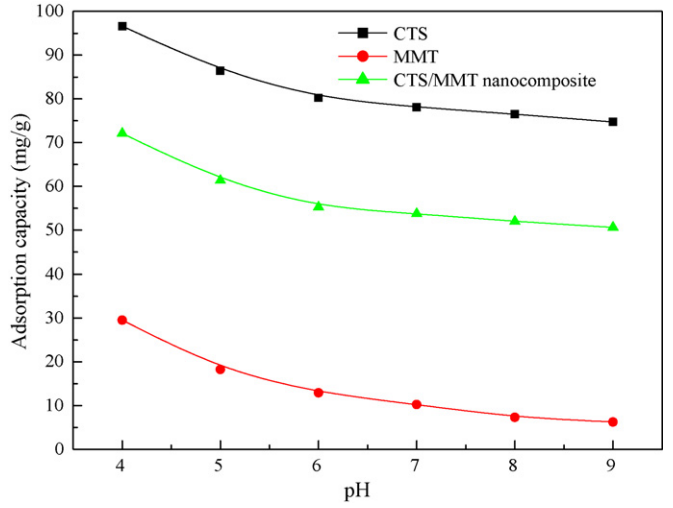

Fig. 5. Effect of the pH values on adsorption capacity of CTS, MMT and the nanocomposite for CR. Adsorption experiments—dye concentration: 400 mg/L; sample dose: 0.1 g/25.00 mL; pH range: 4–9; temperature: 30 °C; equilibrium time: 720 min.

3.5. Effect of temperature on adsorption

Fig. 6 shows the relationship between the temperature and the adsorption capacity of CR by the nanocomposite. The adsorption capacity of the nanocomposite increased with increasing of the temperature from 30 to 50 °C. It is found that the higher temperature is to the advantage of adsorption and that the adsorp-

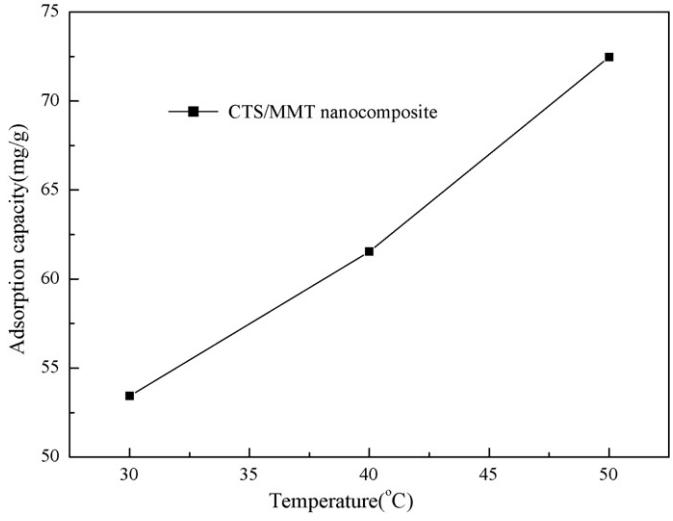

Fig. 6. Effect of the temperature on adsorption capacity of the nanocomposite for CR. Adsorption experiments—dye concentration: 400 mg/L; sample dose: 0.1 g/25.00 mL; pH 7; temperature: 30–50 °C; equilibrium time: 720 min.

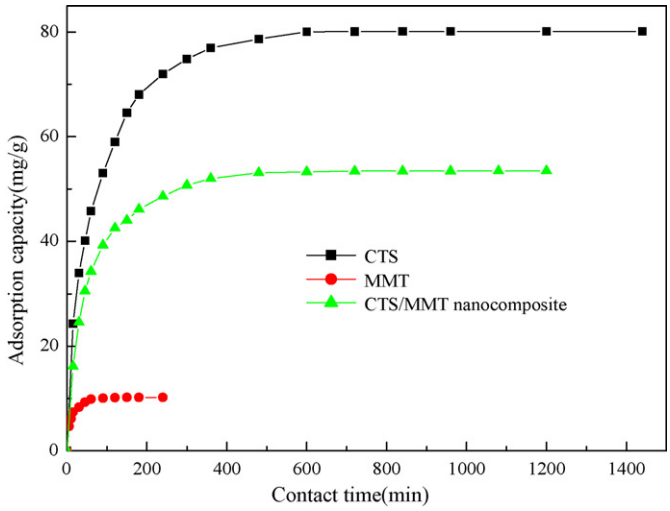

Fig. 7. Effect of the contact time on adsorption capacity of CTS, MMT and the nanocomposite for CR. Adsorption experiments—dye concentration: 400 mg/L; sample dose: 0.1 g/25.00 mL; pH 7; temperature: 30 °C.

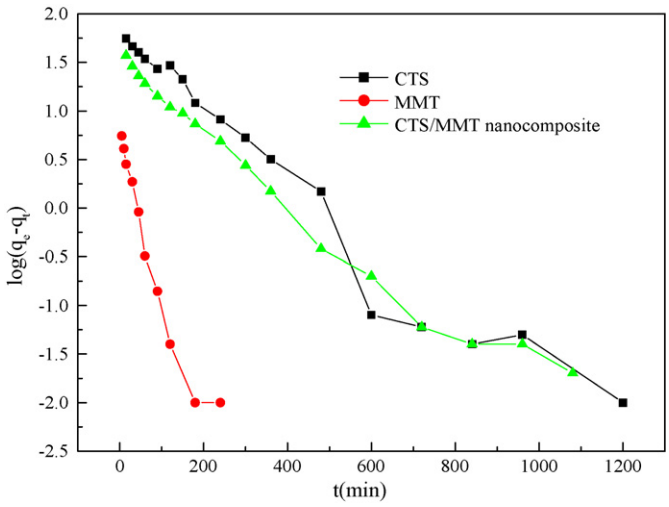

Fig. 8. Pseudo-first-order model for the adsorption of CR by CTS, MMT and the nanocomposite.

tion is an endothermic reaction. The endothermic adsorption has also been reported for the adsorption of CR on activated carbon prepared from coir pith [16] and calcium-rich fly ash [24].

3.6. Adsorption kinetics

Fig. 7 shows the effect of contact time on the adsorption capacities of CR by CTS, MMT and the nanocomposite, respectively. It is clear that the adsorption capacity of CTS, MMT and the nanocomposite increased rapidly in the initial stages of contact time and gradually increased with prolonging the contact time until equilibrium. It can be seen that the adsorption equilibrium of CR on CTS, MMT and the nanocomposite were reached at 600, 120 and 480 min, respectively. So, in the test we choose a adsorption time of 720 min to obtain the adsorption isotherms, which make sure the adsorption equilibrium was reached.

Two simplified kinetic models including pseudo-first-order and pseudo-second-order equations are analysed. A simple kinetic model that describes the process of adsorption is the pseudo-first-order equation. It was suggested by Lagergren [25] for the adsorption of solid/liquid systems and its formula is given as

$$\frac{dq_e}{dt} = k_1(q_e - q_t) \quad (1)$$

where k_1 is the pseudo-first-order rate constant (min^{-1}), q_e and q_t are the amounts of dye adsorbed (mg/g) at equilibrium and at time t (min).

After integration with the initial condition $q_t = 0$ at $t = 0$, Eq. (2) can be obtained:

$$\log(q_e - q_t) = \log q_e - \frac{k_1 t}{2.303} \quad (2)$$

Pseudo-second-order model is based on adsorption equilibrium capacity can be expressed as [26]:

$$\frac{dq_e}{dt} = k_2(q_e - q_t)^2 \quad (3)$$

When the initial condition is $q_t = 0$ at $t = 0$, integration leads to Eq. (4):

$$\frac{t}{q_t} = \frac{1}{k_2 q_e^2} + \frac{t}{q_e} \quad (4)$$

where k_2 ($g\,mg^{-1}\,min^{-1}$) is the rate constant of the pseudo-second-order adsorption. The linear plots of $\log(q_e - q_t)$ versus t and (t/q_t) versus t drawn for the pseudo-first-order and the pseudo-second-order models, respectively. The rate constants k_1 and k_2 can be obtained from the plot of experimental data.

As seen from Figs. 8 and 9, the correlation coefficients (R) of the pseudo-first-order model are 0.979, 0.961 and 0.987 for CTS, MMT and the nanocomposite, respectively. For the pseudo-second-order model, the correlation coefficients (R) are 0.999, 0.999 and 0.999 for CTS, MMT and the nanocomposite, respectively. Therefore, the adsorption of CR on CTS, MMT and the nanocomposite were better described by the pseudo-second-order rather than by the pseudo-first-order. This result

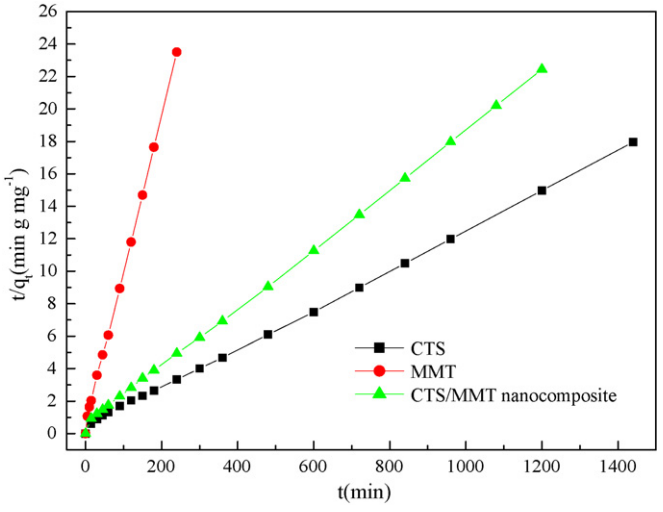

Fig. 9. Pseudo-second-order model for the adsorption of CR by CTS, MMT and the nanocomposite.

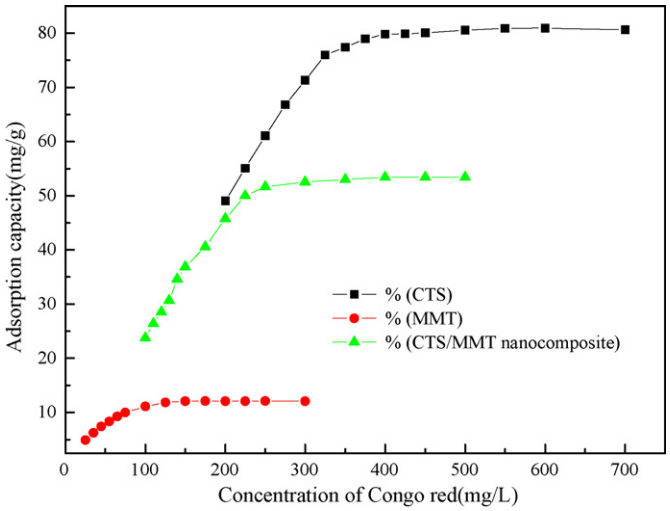

Fig. 10. Effect of the dye concentration on adsorption capacity of CTS, MMT and the nanocomposite for CR. Adsorption experiments—sample dose: 0.1 g/25.00 mL; pH 7; temperature: 30 °C; equilibrium time: 720 min.

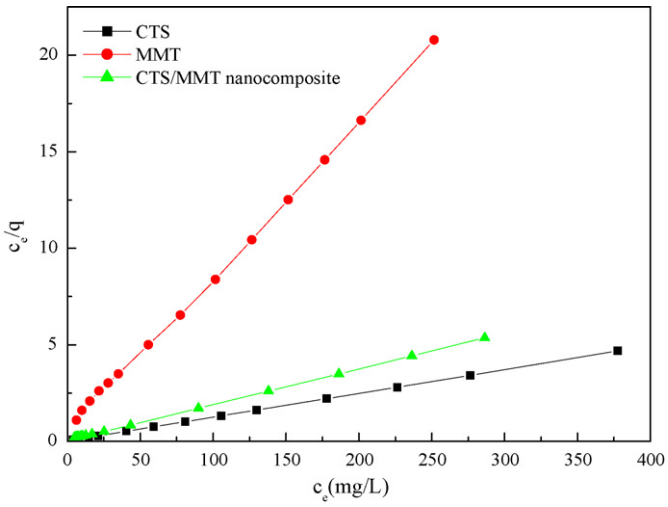

Fig. 11. Langmuir plot for the adsorption of CR by CTS, MMT and the nanocomposite.

also indicates that the adsorption rate of CR dye depends on the concentration of dye at the absorbent surface and the absorbance of these absorbed at equilibrium [27].

3.7. Adsorption isotherms

Fig. 10 shows the adsorption capacity of CR by CTS, MMT and the nanocomposite at different dye concentrations and at 30 °C for samples. The adsorption capacities of CTS, MMT and the nanocomposite increased with increasing of the dye concentration. It can be seen from Fig. 10 that the sharp increase in adsorption capacity from 200 to 325 mg/L, from 25 to 100 mg/L and from 100 to 225 mg/L for CTS, MMT, and the nanocomposite, respectively. However, only a slight increase in the adsorption capacity of CTS, MMT and the nanocomposite can be observed with further increasing the initial concentration of dye.

The amount of dye adsorbed at equilibrium q_e (mg/g) was calculated from the following equation:

$$q_e = \frac{(C_0 - C_e)v}{m} \tag{5}$$

where C_0 (mg/L) is the initial dye concentration, C_e (mg/L) the equilibrium concentration of dye solution, v (L) the volume of dye solution, m (g) is the mass of adsorbent.

The adsorption process can be generally expressed by two isotherm equations, namely, the Langmuir and the Freundlich equations [28], which are represented by the following equations, respectively:

$$\frac{C_e}{q_e} = \frac{1}{bq_m} + \frac{C_e}{q_m} \tag{6}$$

$$q_e = K_f C_e^{1/n} \tag{7}$$

where q_m (mg/g) and b (L/mg) are Langmuir isotherm coefficients. The value of q_m represents the maximum adsorption capacity. K_f (mg/g) and n are Freundlich constants.

The linear plot of C_e/q_e versus C_e drawn for the Langmuir model of the adsorption of CR (Fig. 11). The applicability of the Langmuir isotherm suggests the monolayer coverage of the dye on the surface of CTS, MMT and the nanocomposite. The linearization of the equations and the values of R^2 for CTS, MMT and the nanocomposite are $y = 0.01231x - 0.0225$, 0.999, $y = 0.09539x - 0.7878$, 0.999 and $y = 0.01834x - 0.0843$, 0.999, respectively. The q_m values for the adsorption of CR by CTS, MMT and the nanocomposite were 81.23, 12.70, 54.52 mg/g, respectively, which are same as the experiment data 80.59, 12.10, 53.42 mg/g for CTS, MMT and the nanocomposite, respectively. The adsorption capacity of CTS/MMT nanocomposite for CR was higher than the mean values of those of CTS and MMT. The q_m values for the adsorption of CR by waste Fe(III)/Cr(III) hydroxide, waste orange peel, waste banana pith, biogas waste slurry, waste red mud and paddy straw were 44.00 mg/g [21], 22.44 mg/g [22], 20.29 mg/g [20], 9.50 mg/g [19], 4.05 mg/g [23], 1.01 mg/g [29], respectively. So, the CTS/MMT nanocom-

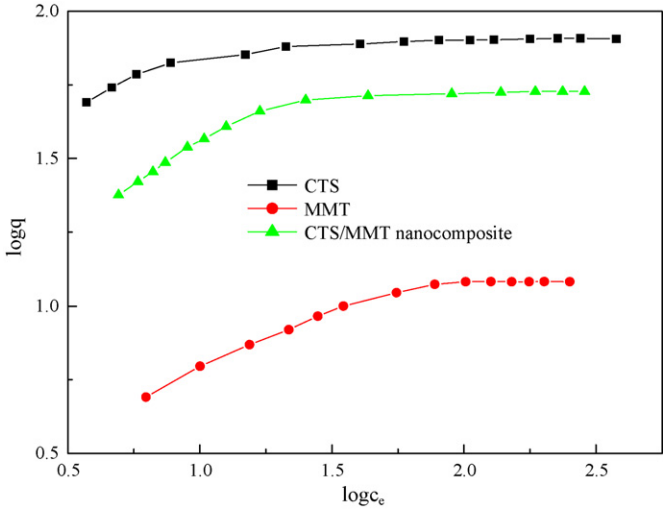

Fig. 12. Freundlich plot for the adsorption of CR by CTS, MMT and the nanocomposite.

posite can be used as an alternative-adsorbing agent in dye wastewaters. Fig. 12 shows that the values of R^2 of Freundlich model for CTS, MMT and the nanocomposite are 0.877, 0.939 and 0.878, respectively. So, the adsorption of CR on CTS, MMT and the nanocomposite do not follow the Freundlich isotherm.

4. Conclusion

The CTS/MMT nanocomposites were prepared by controlling the molar ratios of CTS to MMT. The results show that the CR dye adsorption process is dependent on the molar ratios of CTS to MMT, initial pH value of the dye solution and temperature. The adsorption kinetics obeys the pseudo-second-order model, and the isotherm follows the Langmuir monolayer model. Compared with CTS, the CTS/MMT nanocomposite has well flocculation ability in aqueous solution, comparative low cost and relative high adsorption capacity. Therefore, the nanocomposite can be effectively used as an adsorbent for the removal of CR from wastewaters.

Acknowledgement

This work was financially supported with the Science and Technology Major Project of Gansu Province (no. 2GS052-A52-002-07).

References

[1] E.A. Clarke, R. Anliker, in: O. Hutzinger (Ed.), The Handbook of Environmental Chemistry, Springer-Verlag, Berlin, 1980, p. 181.
[2] M. Mitchell, W.R. Ernst, G.R. Lightsey, Adsorption of textile dyes by activated carbon produced from agricultural, municipal and industrial wastes, Bull. Environ. Contam. Toxicol. 19 (1) (1978) 307–311.
[3] M.Y. Chang, R.S. Juang, Adsorption of tannic acid, humic acid, and dyes from water using the composite of chitosan and activated clay, J. Colloid Interf. Sci. 278 (1) (2004) 18–25.
[4] R.S. Vieira, M.M. Beppu, Interaction of natural and crosslinked chitosan membranes with Hg(II) ions, Colloids Surf. A 279 (1–3) (2006) 196–207.
[5] R.S. Juang, C.Y. Ju, Equilibrium sorption of Copper(II)-ethylenediaminetetraacetic acid chelates onto cross-linked, polyaminated chitosan beads, Ind. Eng. Chem. Res. 36 (12) (1997) 5403–5409.
[6] G. Crini, Non-conventional low-cost adsorbents for dye removal: a review, Bioresour. Technol. 97 (9) (2006) 1061–1085.
[7] C.C. Wang, L.C. Juang, T.C. Hsu, C.K. Lee, J.F. Lee, F.C. Huang, Adsorption of basic dyes onto montmorillonite, J. Colloid Interf. Sci. 273 (1) (2004) 80–86.
[8] A.S. Özcan, A. Özcan, Adsorption of acid dyes from aqueous solutions onto acid-activated bentonite, J. Colloid Interf. Sci. 276 (1) (2004) 39–46.
[9] G. Lagaly, Introduction: from clay mineral-polymer interactions to clay mineral-polymer nanocomposites, Appl. Clay Sci. 15 (1–2) (1999) 1–9.
[10] S.F. Wang, L. Shen, Y.J. Tong, L. Chen, I.Y. Phang, P.Q. Lim, T.X. Liu, Biopolymer chitosan/montmorillonite nanocomposites: preparation and characterization, Polym. Degrad. Stab. 90 (1) (2005) 123–131.
[11] M. Darder, M. Colilla, E. Ruiz-Hitzky, Biopolymer-clay nanocomposites based on chitosan intercalated in montmorillonite, Chem. Mater. 15 (20) (2003) 3774–3780.
[12] M. Darder, M. Colilla, E. Ruiz-Hitzky, Chitosan-clay nanocomposites: application as electrochemical sensors, Appl. Clay Sci. 28 (1–4) (2005) 199–208.
[13] H. Gecol, E. Ergican, P. Miakatsindila, Biosorbent for tungsten species removal from water: effects of co-occurring inorganic species, J. Colloid Interf. Sci. 292 (2) (2005) 344–353.
[14] S.S. Ray, K. Okamoto, M. Okamoto, Structure–property relationship in biodegradable poly(butylenes succinate)/layered silicate nanocomposites, Macromolecules 36 (7) (2003) 2355–2367.
[15] B.S. Inbaraj, C.P. Chiu, G.H. Ho, J. Yang, B.H. Chen, Removal of cationic dyes from aqueous solution using an anionic poly-γ-glutamic acid-based adsorbent, J. Hazard. Mater. 137 (1) (2006) 226–234.
[16] C. Namasivayam, D. Kavitha, Removal of Congo Red from water by adsorption onto activated carbon prepared from coir pith, an agricultural solid waste, Dyes Pigments 54 (1) (2002) 47–58.
[17] Y.S. Ho, Effect of pH on lead removal from water using tree fern as the sorbent, Bioresour. Technol. 96 (11) (2005) 1292–1296.
[18] V.N. Singh, G. Mishra, K.K. Panday, Removal of Congo Red by wollastonite, Indian J. Technol. 22 (1984) 70–71.
[19] C. Namasivayam, R.T. Yamuna, Removal of Congo Red from aqueous solutions by biogas waste slurry, J. Chem. Technol. Biotechnol. 53 (22) (1992) 153–157.
[20] C. Namasivayam, N. Kanchana, Waste banana pith as adsorbent for colour removal from wastewaters, Chemosphere 25 (11) (1992) 1691–1705.
[21] C. Namasivayam, R. Jeyakumar, R.T. Yamuna, Dye removal from wastewater by adsorption on waste Fe(III)/Cr(III) hydroxide, Waste Manage. 14 (7) (1994) 643–648.
[22] C. Namasivayam, N. Muniasamy, K. Gayathri, M. Rani, K. Ranganathan, Removal of dyes from aqueous solutions by cellulosic waste orange peel, Bioresour. Technol. 57 (1) (1996) 37–43.
[23] C. Namasivayam, D.J.S.E. Arasi, Removal of Congo Red from wastewater by adsorption onto waste red mud, Chemosphere 34 (2) (1997) 401–417.
[24] B. Acemioğlu, Adsorption of Congo Red from aqueous solution onto calcium-rich fly ash, J. Colloid Interf. Sci. 274 (2) (2004) 371–379.
[25] S. Lagergren, About the theory of so-called adsorption of soluble substances, Kungliga Svenska Vetenskapsakademiens Handlingar 24 (4) (1898) 1–39.
[26] Y.S. Ho, G. McKay, Pseudo-second order model for sorption processes, Process Biochem. 34 (5) (1999) 451–465.
[27] S.L. Sun, A.Q. Wang, Adsorption kinetics of Cu(II) ions using *N*,*O*-carboxymethyl-chitosan, J. Hazard. Mater. 131 (1–3) (2006) 103–111.
[28] K. Periasamy, C. Namasivayam, Removal of Nickel(II) from aqueous solution and nickel plating industry wastewater industry using an agriculture waste: peanut hull, Waste Manage. 15 (1) (1995) 63–68.
[29] N. Deo, M. Ali, Dye adsorption by a new low cost material: Congo Red. 1, Indian J. Environ. Prot. 13 (7) (1993) 496–508.